A Novel 2D Mn(II) Coordination Polymer Based on the New Flexible 3-Carboxy-1-(4′-(2″-carboxy)biphenylmethyl)-2-oxidopyridinium and the Pyrazino[2,3-*f*][1,10]phenanthroline Ligands

Qian Qiao, Xiao-Min Yu, Yuan-Rui Wang, and Zhen-Yu Li

College of Chemistry and Chemical Engineering, Changchun University of Technology,
Changchun 130012, P. R. China

Reprint requests to Prof. Qian Qiao. E-mail: qiaoqianccut@yahoo.com.cn

Z. Naturforsch. **2013**, *68b*, 155 – 160 / DOI: 10.5560/ZNB.2013-2276
Received October 16, 2012

A novel 2D coordination polymer, [Mn(pyphen)(L)] (**1**) (L = 3-carboxy-1-(4′-(2″-carboxy)biphenylmethyl)-2-oxidopyridinium and pyphen = pyrazino[2,3-*f*][1,10]phenanthroline), has been synthesized under hydrothermal conditions, and characterized by elemental analysis, IR, UV/Vis spectra and its optical band gap. Crystal data for **1**: $C_{34}H_{21}MnN_5O_5$, monoclinic, space group $P2_1/c$, $a = 12.484(4)$, $b = 13.473(5)$, $c = 16.479(3)$ Å, $\beta = 99.618(6)°$, $V = 2732.8(14)$ Å^3, $Z = 4$. In **1**, each L ligand coordinates to three Mn(II) atoms through its two carboxylate groups and one phenolate unit. In this way, L^{2-} ligands link neighboring Mn(II) atoms to generate a layer structure.

Key words: Crystal Structure, Coordination Polymer, 3-Carboxy-1-(4′-(2″-carboxy)biphenylmethyl)-2-oxidopyridinium, Pyrazino[2,3-*f*][1,10]phenanthroline

Introduction

The rational design and assembly of coordination polymers are of current interest because of their fascinating topologies and potential applications in gas storage, luminescence, separation, catalysis, magnetism, drug delivery, and so on [1 – 5]. It is well known that the structures of coordination polymers are dependent on several factors, such as the organic anions, metal cations, *N*-donor ligands, pH values, and reaction temperatures [6 – 10]. Among these, the organic anions play an important role in the construction of coordination polymers with fascinating architectures [11 – 13]. Polycarboxylate ligands are good candidates for the construction of coordination polymers and have arisen a good deal of interest [14]. So far, benzene-multicarboxylate ligands, such as 1,4-benzenedicarboxylate, 1,3-benzenedicarboxylate and 1,3,5-benzenetricarboxylate, have been widely used in the construction of coordination polymers owing to their versatile coordination behaviors [15 – 17]. However, less attention has been paid to the *N*-heteroaromatic carboxylates involving a pyridinium core. On the basis of the above consideration, we synthesized the flexible dicarboxylic acid ligand 3-carboxy-1-(4′-(2″-carboxy)biphenylmethyl)-2-oxidopyridinium (H_2L) (Fig. 1). The L^{2-} ligand has two carboxylate and one phenolate group at terminal position, therefore it can show varying coordination behaviors. On the other hand, the phenolate oxygen atom of the L^{2-} ligand can also be involved in the formation of intramolecular hydrogen bonds, stabilizing the whole structure.

In this work, a novel 2D coordination polymer [Mn(pyphen)(L)] (**1**) has been synthesized under hydrothermal conditions. Its structure has been determined by single-crystal X-ray diffraction analysis, and the compound was characterized by elemental analy-

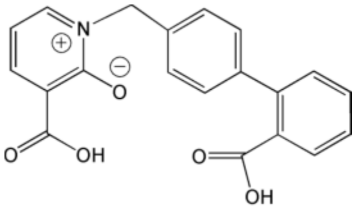

H_2L

Fig. 1. The H_2L ligand precursor used in this work.

sis, IR and UV/Vis spectroscopy, and its optical band gap.

Results and Discussion

*Structure description of **1***

Selected bond lengths and angles for [Mn(pyphen)(L)] (**1**) are listed in Table 1. The asymmetric unit of **1** consists of one Mn(II) dication, one L^{2-} dianion, and one pyphen ligand. As shown in Fig. 2, each Mn(II) atom is six-coordinated by two nitrogen atoms from one pyphen ligand (Mn(1)–N(1) = 2.291(3) and Mn(1)–N(2) = 2.319(3) Å) and four oxygen atoms from two L^{2-} dianions (Mn(1)–O(1) = 2.100(2), Mn(1)–O(4)^{i} = 2.176(2), Mn(1)–O(3)^{ii} = 2.183(2) and Mn(1)–O(4)^{ii} = 2.247(2) Å) in a distorted octahedral coordination geometry (for symmetry operations used see Table 1). Two nitrogen atoms (N1, N2) and two oxygen atoms (O1, O4^{ii}) constitute the equatorial plane, while two more oxygen atoms (O3^{i}, O4^{i}) occupy the axial positions. The Mn–O bond lengths are close to the reported ones found in the related compound $[\text{Mn(L1)(H}_2\text{O)}_2]_n$ ($\text{H}_2\text{L1}$ = 5-carboxyl-1-carboxymethyl-3-oxidopyridinium) [18] In **1**, each L ligand coordinates with three Mn(II) atoms through its two carboxylate and one phenolate groups. Two carboxylates bridge two Mn(II) atoms

Bond lengths			
Mn(1)–O(1)	2.100(2)	Mn(1)–O(4)^{i}	2.176(2)
Mn(1)–O(3)^{ii}	2.183(2)	Mn(1)–O(4)^{ii}	2.247(2)
Mn(1)–N(1)	2.291(3)	Mn(1)–N(2)	2.319(3)
Bond angles			
O(1)–Mn(1)–O(4)^{i}	97.98(9)	O(1)–Mn(1)–O(3)^{ii}	95.25(9)
O(4)^{i}–Mn(1)–O(3)^{ii}	147.44(8)	O(1)–Mn(1)–O(4)^{ii}	95.17(9)
O(4)^{i}–Mn(1)–O(4)^{ii}	72.27(9)	O(3)^{ii}–Mn(1)–O(4)^{ii}	77.02(8)
O(1)–Mn(1)–N(1)	95.14(9)	O(4)^{i}–Mn(1)–N(1)	125.25(9)
O(3)^{ii}–Mn(1)–N(1)	82.70(9)	O(4)^{ii}–Mn(1)–N(1)	157.97(9)
O(1)–Mn(1)–N(2)	164.68(9)	O(4)^{i}–Mn(1)–N(2)	95.76(9)
O(3)^{ii}–Mn(1)–N(2)	76.44(9)	O(4)^{ii}–Mn(1)–N(2)	95.42(9)
N(1)–Mn(1)–N(2)	71.28(9)		

Table 1. Selected bond lengths (Å) and angles (deg) for **1** with estimated standard deviations in parentheses[a].

[a] Symmetry transformations used to generate equivalent atoms: ^{i} $-x+1$, $y+1/2$, $--z+3/2$; ^{ii} x, $-y+1/2$, $z-1/2$.

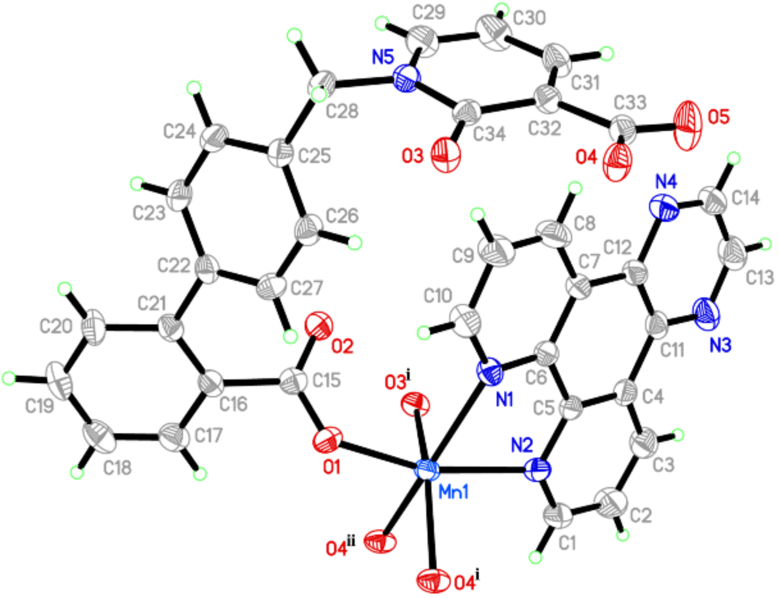

Fig. 2 (color online). ORTEP view of **1** showing the local coordination environment of the Mn(II) center (40 % probability displacement ellipsoids).

to give a dinuclear Mn(II) unit (Fig. 3). In this way, L ligands link neighboring Mn(II) atoms to generate a layer structure (Fig. 3). In the layer, two pairs of L ligands form strong π-π stacking interactions (centroid-to-centroid distance of *ca.* 3.63 Å and face-to-face distance of *ca.* 3.51 Å) (Fig. 4). These π-π stacking interactions further stabilize the 2D structure of **1**. From a topological perspective, if each Mn(II) dimer can be regarded as a 4-connected node, and each L^{2-} dianion can be considered as a connector, the layer can be described as a (4,4) network (Fig. 5). As shown in Fig. 6, the adjacent layers are stacked in an ABC fashion.

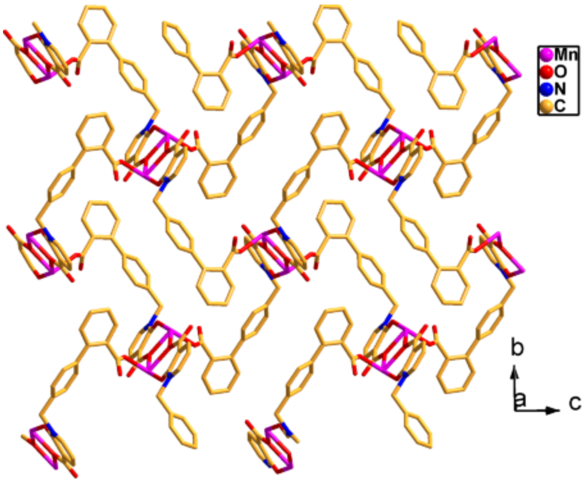

Fig. 3 (color online). View of the layer structure of **1** (pyphen ligands are omitted for clarity).

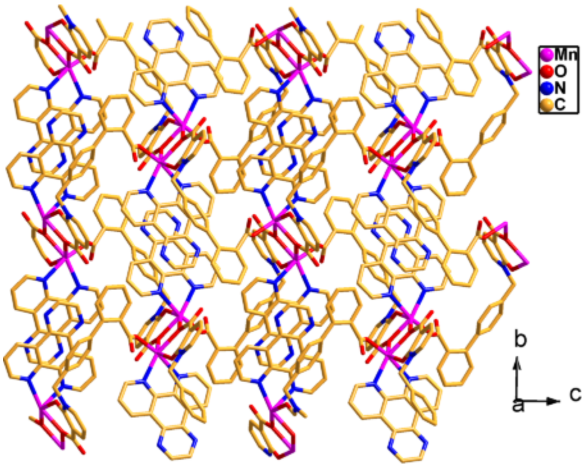

Fig. 4 (color online). View of the layer structure of **1**.

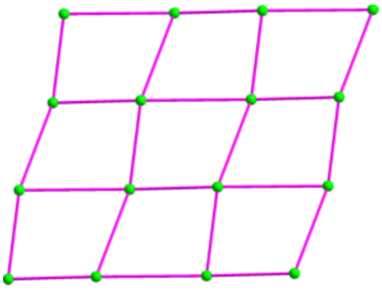

Fig. 5 (color online). Schematic representation of the 2D (4,4) network of **1**.

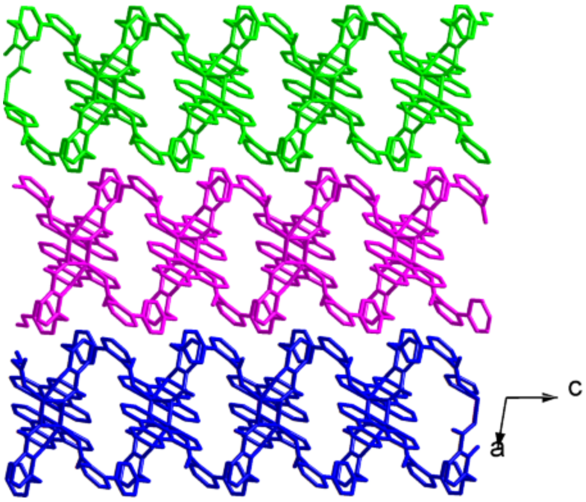

Fig. 6 (color online). View of the stacking mode of neighboring layers of **1**.

It should be pointed out that although some coordination polymers based on 1,10-phenanthroline derivatives have been reported, examples constructed by *N*-heteroaromatic carboxylates involving a pyridinium core and 1,10-phenanthroline derivatives have never been observed. It is noteworthy that the structure of **1** is entirely different from that of the related compound $[Mn(L1)(H_2O)_2]_n$ [18], where $L1^{2-}$ ligands link neighboring Mn(II) atoms into a 3D pillared-layer framework with left- and right-handed helical chains.

IR spectrum of 1

For compound **1**, the asymmetric stretching vibrations of the carboxylate groups of the L^{2-} dianions [$\nu_{as}(COO)$] appear at 1660 and 1597 cm^{-1}, and its symmetric stretching vibrations [$\nu_s(COO)$] at 1577 and 1544 cm^{-1}. Their differences $\Delta\nu[\nu_{as}(COO)$–

ν_s(COO)] are 63 and 33 cm^{-1}, respectively, suggesting the existence of two coordination modes (monodentate and bidentate) for the carboxylate groups in the compound. The peak of 1484 cm^{-1} can be assigned to the C=N stretching vibration of the *N*-donor pyphen ligand.

UV/Vis absorption spectrum of ***1***

Fig. 7 shows the UV/Vis absorption spectrum of **1** obtained in the crystalline state at room temperature. The shoulders from 400 to 500 nm are assigned to the *d-d* spin-allowed transitions of the Mn(II) ion. The lower energy band from 250 to 300 nm can be considered as $\pi^* \rightarrow \pi$ transitions of the ligand.

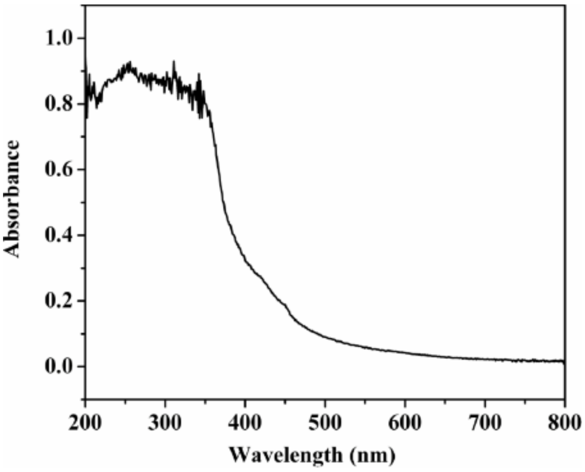

Fig. 7 (color online). UV/Vis absorption spectrum of **1**.

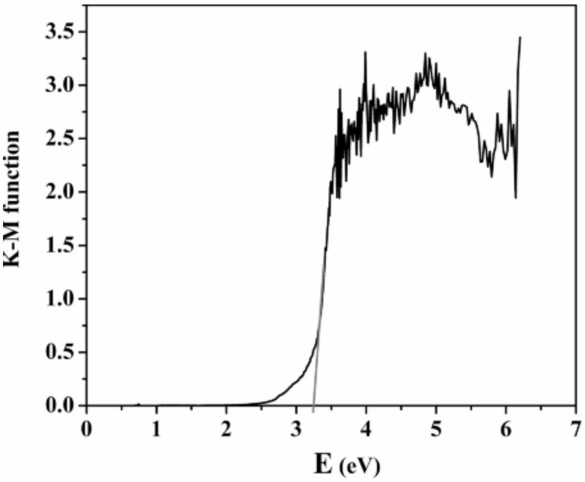

Fig. 8 (color online). Kubelka-Munk-transformed diffuse reflectance spectrum of **1**.

Optical band gaps of ***1***

Some coordination polymers have been reported to be promising semiconductive materials [19]. Encouraged by this, the conductivity potential of compound **1** was investigated. The diffuse reflectivity for **1** was measured to get its band gap (E_g), which was defined as the intersection point between the line extrapolated from the linear portion of the adsorption edge in a plot of the Kubelka-Munk function F *versus* the energy E and the energy axis. The Kubelka-Munk function, $F = (1-R)^2/2R$, was transformed from the recorded diffuse reflectance data, where R is the reflectance of an infinitely thick layer at a given wavelength. The F against E plot is illustrated in Fig. 8. The E_g value assessed from the steep absorption edge for compound **1** is 3.24 eV, which indicates that compound **1** is a potential semiconductive material.

Magnetic properties of ***1***

The temperature-dependent magnetic susceptibility data of compound **1** have been measured at an applied magnetic field of 1 kOe (1 kOe = 7.96×10^4 A m^{-1}) in the temperature range of 2 – 300 K (Fig. 9). For **1**, the $\chi_m T$ value at 300 K is 3.93 cm^3 mol^{-1} K, which is lower than the expected value of 4.38 cm^3 mol^{-1} K expected for uncoupled Mn(II) ions ($S = 5/2$ and $g = 2$) [20]. Upon cooling, the values keep almost constant from 300 to 40 K (3.83 cm^3 mol^{-1} K), and then

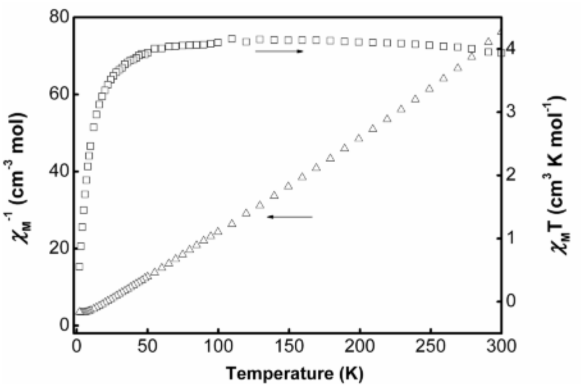

Fig. 9. Plots of the temperature dependence of $\chi_m T$ (open squares) and χ_m^{-1} (open triangles) for compound **1**.

quickly reach a minimum value of 0.55 $cm^3\,mol^{-1}$ K at 2 K. This feature shows the occurrence of a weak antiferromagnetic interactions between the Mn(II) ions of the dinuclear units.

Experimental Section

General

All materials were of analytical or reagent grade and used as received without further purification. Elemental analysis was carried out with a Perkin-Elmer 240C analyzer. The FT-IR spectra were recorded from KBr pellets in the range 4000 – 400 cm^{-1} on a Mattson Alpha-Centauri spectrometer. Diffuse reflectivity was measured from 200 to 800 nm using barium sulfate as a standard of reflectance. Temperature-dependent magnetic susceptibility data for compound **1** were measured on a Quantum Design MPMSXL SQUID magnetometer under an applied field of 1 kOe over the temperature range of 2 – 300 K.

Synthesis of compound 1

H_2L was synthesized according to the literature [21 – 23]. A mixture of $MnCl_2{\cdot}4H_2O$ (0.5 mmol), pyphen (0.5 mmol) and H_2L (0.5 mmol) was dissolved in 12 mL distilled water. The pH value of the system was adjusted to between 4.5 and 5.5 by addition of triethylamine. The resulting mixture was sealed in a 23 mL Teflon-lined stainless-steel autoclave and heated at 423 K for 3 d under autogeneous pressure. After the mixture was cooled to room temperature at a rate of 10 °C h^{-1}, crystals of **1** were obtained. Yield: 21 % based on Mn(II). – Anal. for $C_{34}H_{21}MnN_5O_5$ (%): calcd. C 64.36, H 3.34, N 11.04; found C 64.22, H 3.51, N 10.93. – IR (KBr, cm^{-1}): ν = 1660s, 1597s, 1577s, 1544s, 1484m, 1439w, 1389w, 1356m, 1213w, 1168w, 1118w, 1080w, 1064w, 997w, 931w, 815w, 776m.

X-Ray structure determination

Single-crystal X-ray diffraction data for **1** were recorded on an Oxford Diffraction Gemini R Ultra diffractometer with graphite-monochromatized MoK_α radiation ($\lambda = 0.71073$ Å) at 293 K. The structure was solved by Direct Methods with SHELXS-97 [24, 25] and refined by full-matrix least-squares techniques using the SHELXL-97 [26, 27] program. Non-hydrogen atoms were refined with anisotropic displacement parameters. Carbon-bound hydrogen atoms were generated geometrically. Details are summarized in Table 2.

Table 2. Crystal structure data for **1**.

Formula	$C_{34}H_{21}MnN_5O_5$
M_r	634.50
Crystal size, mm^3	0.22 × 0.18 × 0.16
Crystal system	monoclinic
Space group	$P2_1/c$
a, Å	12.484(4)
b, Å	13.473(5)
c, Å	16.479(3)
β, deg	99.618(6)
V, $Å^3$	2732.8(14)
Z	4
D_{calcd}, g cm^{-3}	1.54
μ(MoK_α), mm^{-1}	0.5
F(000), e	1300
hkl range	$-14 \le h \le 13$; $-11 \le k \le 16$; $-14 \le l \le 19$
θ range, deg	2.93 – 25.03
Refl. collect. / unique / R_{int}	9537 / 4793 / 0.0373
Data / ref. parameters	4793 / 406
$R1$ / $wR2$ [$I > 2\sigma(I)$]	0.0480 / 0.0982
$R1$ / $wR2$ (all data)	0.0743 / 0.1122
GoF (F^2)	1.021
$\Delta\rho_{max/min}$, e $Å^{-3}$	0.43 / – 0.35

CCDC 905828 (**1**) contains the supplementary crystallographic data for this paper. These data can be obtained free of charge from The Cambridge Crystallographic Data Centre *via* www.ccdc.cam.ac.uk/data_request/cif.

Acknowledgement

This work was supported by the National Science Foundation of China (no. 21171026).

[1] M. O'Keeffe, M. A. Peskov, S. J. Ramsden, O. M. Yaghi, *Acc. Chem. Res.* **2008**, *41*, 1782 – 1789.

[2] G. Feìrey, *Chem. Soc. Rev.* **2008**, *37*, 191 – 214.

[3] S. Horike, S. Shimomura, S. Kitagawa, *Nature Chem.* **2009**, *1*, 695 – 704.

[4] S. R. Batten, K. S. Murray, *Coord. Chem. Rev.* **2003**, *246*, 103 – 130.

[5] H. Wu, J. Yang, Z. M. Su, S. R. Batten, J. F. Ma, *J. Am. Chem. Soc.* **2011**, *133*, 11406 – 11409.

[6] J.-R. Li, R. J. Kuppler, H.-C. Zhou, *Chem. Soc. Rev.* **2009**, *38*, 1477 – 1504.

[7] Y.-S. Bae, O. K. Farha, A. M. Spokoyny, C. A. Mirkin, J. T. Hupp, R. Q. Snurr, *Chem. Commun.* **2008**, 4135 – 4137.

[8] J. An, S. J. Geib, N. L. Rosi, *J. Am. Chem. Soc.* **2010**, *132*, 38 – 39.

[9] L. Ma, C. Abney, W. Lin, *Chem. Soc. Rev.* **2009**, *38*, 1248 – 1256.

[10] H. Wu, H. Y. Liu, Y. Y. Liu, J. Yang, B. Liu, J. F. Ma, *Chem. Commun.* **2011**, *47*, 1818 – 1820.

[11] F. Nouar, J. F. Eubank, T. Bousquet, L. Wojtas, M. J. Zaworotko, M. Eddaoudi, *J. Am. Chem. Soc.* **2008**, *130*, 1833 – 1835.

[12] V. A. Blatov, L. Carlucci, G. Ciani, D. M. Proserpio, *CrystEngComm* **2004**, *6*, 377 – 395.

[13] Z.-L. Xu, Y. He, H.-L. Wang, *Z. Naturforsch.* **2011**, *66b*, 1 – 6.

[14] Q. Qiao, R. Wang, G. Wu, T. Tang, *Cryst. Res. Technol.* **2009**, *44*, 567 – 570.

[15] X.-Y. Wang, S. Ma, T. Li, S. W. Ng, *Z. Naturforsch.* **2011**, *66b*, 103 – 106.

[16] Z.-G. Kong, X.-Y. Ma, Z.-L. Xu, *Z. Naturforsch.* **2010**, *65b*, 1173 – 1176.

[17] M.-L. Xu, R. Zhou, G.-Y. Wang, S. W. Ng, *Acta Crystallogr.* **2008**, *E64*, m712–m713.

[18] M.-X. Jiang, C.-H. Zhan, Y.-L. Feng, Y.-Z. Lan, *Cryst. Growth Des.* **2010**, *10*, 92 – 98.

[19] H. S. Liu, Y. Q. Lan, S. L. Li, *Cryst. Growth Des.* **2010**, *10*, 5221 – 5226.

[20] K. O. Kongshaug, H. Fjellvåg, *Polyhedron* **2007**, *26*, 5113 – 5119.

[21] G.-Q. Kong, C.-D. Wu, *CrystEngComm* **2012**, *14*, 847 – 852.

[22] N. A. Caplan, C. I. Pogson, D. J. Haynes, G. M. Blackburn, *J. Chem. Soc., Perkin Trans.* **2000**, *1*, 421 – 437.

[23] G. Yucesan, M. H. Yu, C. J. O'Connor, J. Zubieta, *CrystEngComm* **2005**, *7*, 711 – 721.

[24] G. M. Sheldrick, SHELXS-97, Program for the Solution of Crystal Structures, University of Göttingen, Göttingen (Germany) **1997**.

[25] G. M. Sheldrick, *Acta Crystallogr.* **1990**, *A46*, 467 – 473.

[26] G. M. Sheldrick, SHELXL-97, Program for the Refinement of Crystal Structures, University of Göttingen, Göttingen (Germany) **1997**.

[27] G. M. Sheldrick, *Acta Crystallogr.* **2008**, *A64*, 112 – 122.